

M. A. MOLINE and M. J. OLIVER, University of Delaware, USA, C. ORRICO and R. ZANEVELD, WetLabs Inc., USA and I. SHULMAN, Naval Research Laboratory, USA

DOI: 10.1533/9780857093523.2.134

Abstract: This chapter begins with a brief introduction to the generation of light in bioluminescence in marine organisms, the uses of bioluminescence, and the distribution of bioluminescence in the ocean. The chapter then focuses on the instrumentation designed to measure bioluminescence and the propagation of bioluminescence in and out of the water column. Two case examples are used to illustrate current approaches to the propagation bioluminescence and the incorporation of these techniques into hydrodynamic models. The chapter ends with applications and future directions for bioluminescence research.

Key words: bioluminescence, bathyphotometer, ecological modeling, optical detection, bioluminescence leaving radiance, point source.

7.1 Introduction

‘... when you strike the sea with a rod by night and the water is seen to shine.’
Aristotle, 350 BC

There is a long documented history by seafarers, philosophers, poets, and scientists of their fascination with brilliant displays of bioluminescence in the wakes of ships, breaking waves, around the bodies of rapidly moving fish and mammals, and from simple agitation of the water with one’s hand or a stick. Bioluminescence in the ocean is the result of biologically-generated photons from a chemiluminescent reaction. It is produced by a range of small single cell bacteria to large vertebrates representing over 700 genera and 16 phyla (Herring, 1987). The ubiquitous feature of most of these organisms is that mechanical stimulation will cause them to generate light. The reasons for these luminous displays appear to be as varied as the organisms themselves, but may be divided into basic categories of predator avoidance, prey attraction, physiological maintenance, and intra-species communication (Abrahams and Townsend, 1993; Burkenroad, 1943; Morin, 1983; Morin and Cohen, 1991, 2010). The wonder and curiosity of these displays were primary

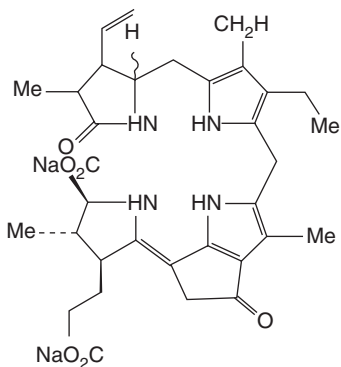
drivers for much of the early research on this phenomenon to understand the physiological mechanisms for bioluminescence, as well as the ecological advantage that bioluminescent abilities provides to these luminous organisms (Alberte, 1993). While current exploration of these topics continues, the genetic basis for and evolution of bioluminescence, physiological trade-offs of bioluminescence, and the synthesis pathways for the light-producing substrates are currently a focus of basic research. In addition to these lines of investigation, the fact that these organisms produce light upon mechanical stimulation is an obvious military concern that has motivated a long history of inquiry attempting to understand the mechanisms driving the horizontal and vertical distributions of bioluminescence in the ocean (OSB/NRC, 1997; Wren and May, 1997). There is a number of excellent recent reviews on the subject of bioluminescence (see Haddock *et al.*, 2010; Widder 2010), which are largely centered on the organismal aspects of the phenomena (evolution, ecology, biodiversity, chemistry). As this is a volume on subsea optics, we tailor this review to focus on the light production, the measurement of bioluminescence, and the propagation of bioluminescent light within and out of the ocean. This is a similar approach to a volume entitled ‘Optical aspects of oceanography’ by Jerlov and Nielsen (1974), which included a chapter by Boden and Kampa (1974) on bioluminescence. After a brief background of the general aspects of bioluminescence, a detailed description of the measurement approaches and results from those observations will be followed by two case studies that address the propagation of broadband bioluminescence in optically dynamic oceanic waters. Finally, a review of some hydrodynamic modeling efforts using bioluminescence and future directions will be discussed.

7.1.1 Diversity of light-producing reactions

‘Phosphorescence is the result of a chemical action under the control of the animal but in certain inferior animals (infusories et annelides) the production of light is a spontaneous act of the animal, manifest on irritation by chemical or mechanical means.’

A. C. Becquerel, 1844

Bioluminescence is the generation of photons resulting from an energy release from a chemical reaction. In the majority of organisms, light is emitted from the oxidation of luciferin molecules. There are different forms of luciferin, which are dependent on the organism. For example, in the case of dinoflagellates, luciferin is a tetrapyrrol ring structure similar to precursors of both chlorophyll and heme (Fig. 7.1). Other common luciferin molecules include bacterial luciferin, *Cypridina* luciferin, and coelenterazine. The oxidation rate of luciferin, and thus the production of light, is system dependent,



7.1 The tetrapyrrol structure of dinoflagellate luciferin with general reaction to produce bioluminescence. (Source: From Nakamura *et al.*, 1989.)

but generally controlled by either an enzyme luciferase or a photoprotein bound to luciferin. In the case of the photoprotein, the production is not a direct oxidation of luciferin, but rather also dependent on the binding of a cation or cofactor (i.e. Ca^{2+}). In addition, the ability of the organism to supply these substrates and catalyst also governs the rate of reactions, and those have been found to be dependent, among other things, on diet (Haddock *et al.*, 2001), photosynthetic rates (autotrophs), pH within the light organ-elles (Smith *et al.*, 2011), the interaction with the host in the case of symbi-onts, and the organism's ability to maintain the synthetic pathways of the luciferins, processes that remain largely unknown (see Widder, 2010).

As mentioned, much of the variety seen in these reactions is dependent on the diversity of organisms displaying bioluminescence. The major groups of marine organisms known to be bioluminescent are bacteria, dinoflagellates, radiolarians, cnidarians, ctenophores, cephalopods, ostracods, copepods, euphausiids, decapod shrimps, chetognaths, and fish. While most produce the luciferins and enzymes, others such as some squid species and fish are hosts to symbiotic bioluminescent bacteria. As the biosynthetic pathways are not yet known for any of the marine luciferins, tracing their origins remains a mystery. While luciferins are generally conserved, luciferases and photopro- teins are unique and derived from many evolutionary lineages. For exam- ple, in bioluminescent cnidarians, all use luciferin coelenterazine but differ in the catalyst; photoproteins (hydrozoans), primarily luciferases (scypho- zoans), and unrelated luciferases sometimes in conjunction with luciferin- binding proteins in the case of anthozoans (Haddock *et al.*, 2010). Based on

the taxonomic diversity and the variations in chemical reactions, the evolution of bioluminescence is thought to have occurred independently at least 40 times (Haddock *et al.*, 2010). Explanations for these events are based on both physiological and behavioral mechanisms. The luciferin substrates may have developed from the need to quench oxidative stress from photochemistry. As vision-dependent or light-sensing organisms adapted to and filled niche space deeper in the ocean, the concomitant reduction in oxidative stress changed the role of the molecule to one with chemiluminescent properties (Rees *et al.*, 1998). Natural selection may have also played a large role in the evolution of bioluminescence in the ocean as the migration of species to greater depths selected for enhanced visibility and production of light-producing molecules (Seliger, 1993).

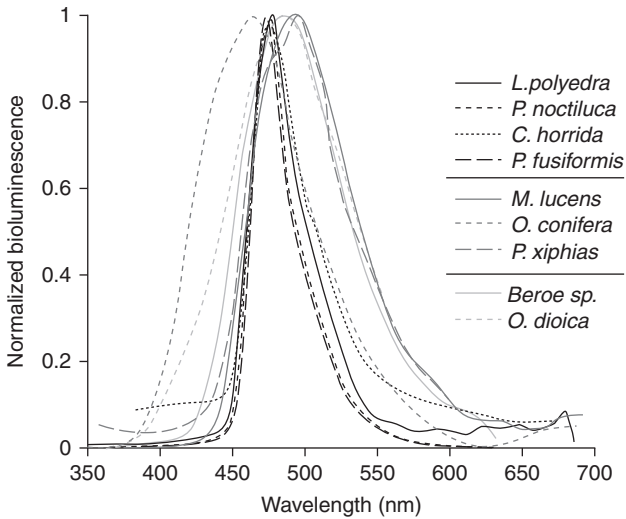
The taxonomic diversity of light emitting organisms produces an analogous number of varied displays and light qualities that are important to consider when measuring bioluminescence (Section 7.2). Bacteria can produce a continuous glow of bioluminescence, known as ‘milky seas’. As symbionts, bacterial-derived light in light organs can be physically modulated by the host (i.e. fishes) using muscles and optical components that change the angular distribution, wavelength, and frequency of display. Many organisms (e.g. dinoflagellates, copepods, cnidarians, and ctenophores) produce individual or multiple flashes that last for varying durations. Some crustaceans, squid, jelly fish, and fish eject the components of the light reaction into the surrounding water, producing bioluminescent clouds. Bioluminescence also occurs in particular location on organism’s bodies and can mimic the downwelling light field from below, effectively removing any downwelling silhouette.

Bioluminescent light fills the visible spectrum from 410 to 710 nm, with the emitted wavelengths again dependent on the organism. Most of the bioluminescent light produced in the ocean is centered in the blue wavelengths (Fig. 7.2), but there are species of annelids and fish that emit light in the yellow and red regions of the spectrum (see Widder, 2010). The differences in wavelength are a result of the conformational differences in the types of luciferin, binding-protein configurations, and the physical make-up of the light structures. Bioluminescence emissions are broadband, with the full width half maximum on the order of 50–100 nm and often skewed to the red (Fig. 7.2). These differences in displays form the basis for understanding the functional roles of bioluminescence in the ocean.

7.1.2 Functional roles of bioluminescence

‘In some places nearly everything brought up seems to emit light and the mud was perfectly full of luminous spaces. ... It is difficult to doubt that in a sea swarming with predaceous crustaceans phosphorescence must be a fatal gift.’

Charles Wyville Thomson, 1870



7.2 Spectral differences in nine commonly occurring bioluminescent species. The four species indicated with black lines are dinoflagellates, while the dark gray are copepods and the light gray lines show *Beroe* sp., a ctenophore, and *Oikopleura dioica*, an appendicularian. While dinoflagellates are closely centered at ~475 nm, high trophic levels show a larger range of color.

Derived from these multiple evolutionary events, the chemical and taxonomic diversity of bioluminescence, and the variations of bioluminescent displays, comes the complexity of the roles bioluminescence play in the ocean. While only briefly summarized here, Haddock *et al.* (2010) is recommended for further reading as it provides one of the most comprehensive summaries on the topic to date. Through the process of selection, one would assume that the ability of organisms to produce bioluminescence, in fact, provides an advantage of some kind. Observations and experimentation have identified and number of advantages, which can be categorized into three general areas: defense, offense, and attraction/recognition. From a defensive perspective, organisms have an array of different bioluminescent mechanisms. Bioluminescence can simply startle potential predators in what is a largely dark environment. As mentioned, bioluminescence can be used as counter-illumination to camouflage the silhouette of organisms from would be predators. Organisms can shed either body parts, in the case of some squid and siphonophores, or a luminescent tag, as in pelagic sea cucumbers and polychaetes. Some organisms eject a cloud of bioluminescence into the water to distract predators for the time needed to escape. Others also cover the predator with a bioluminescent slime to mark the predators for secondary predators (Haddock *et al.*, 2010; Widder, 2002). One of the best

known defensive hypothesis is known as the ‘burglar alarm’, whereby predators/grazers of bioluminescent dinoflagellate are themselves lit up by their prey for detection by secondary predators (Mensing and Case, 1992). The offensive uses that provide an advantage to predators are bioluminescent lures, either physically attached to the organism (i.e. anglerfish) or external organisms in the case of large predators (Haddock *et al.*, 2010). In addition to luring, bioluminescence is used to light up prey (i.e. flashlight fish). Bioluminescence is also found used as a tool to stun offensively.

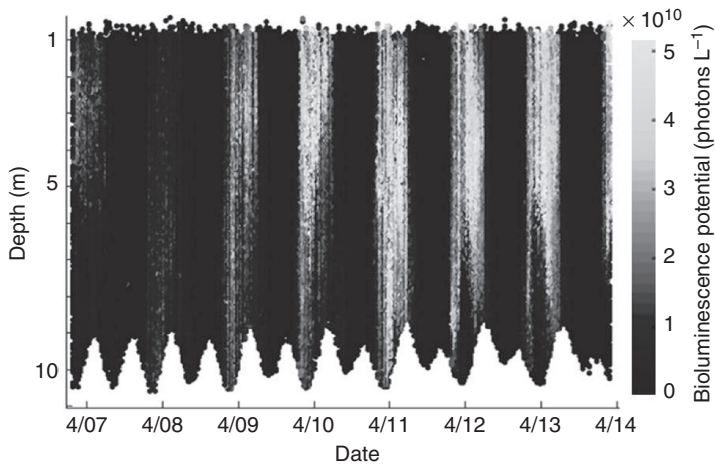
The third advantage afforded to bioluminescent organisms is their ability to enhance communication through light emission. Morin and Bermingham (1980) demonstrated that ostracods use bioluminescence in communication, and have shown experimentally that bioluminescence is used as a form of sexual selection in ostracods (Morin and Cohen, 2010). The males in particular species will secrete luminescence in a vertical pattern over species-specific habitats to attract females, which do not have the ability to bioluminesce (Rivers and Morin, 2008). Fishes also have been shown to use bioluminescent light for communication (Haddock *et al.*, 2010).

7.1.3 Diel changes in oceanic bioluminescence

‘That the burning or glittering light of the Sea did show to us, as though all the Sea our had been burning flames of fire; and all the night long, the Moon being down, you might see to read in any book by the light thereof.’

John Davis, 1598

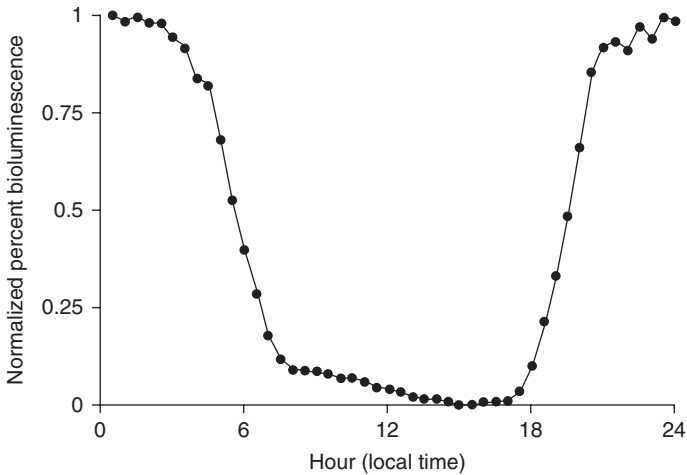
In the measurement of bioluminescence in the ocean (Section 7.2), it is important to understand the numerous influences that community structure, the abundance of the bioluminescent organisms, and the time dependent changes in bioluminescence have on the overall signal. Time dependent changes in *in situ* bioluminescence have been known for some time (Kampa and Boden, 1953); however, Batchelder *et al.* (1990) summarize the integrated effect in the Sargasso Sea of these influences. He found the overall bioluminescence signal in the euphotic zone was a combination of circadian rhythm in dinoflagellate bioluminescence, the release of bioluminescence from photoinhibition, and the change in organism abundance in the surface due to diurnal vertical migration (DVM). There are numerous studies on the circadian rhythm of dinoflagellate bioluminescence (see Morse *et al.*, 1990) and these have shown that the physiological clock is often independent of environmental queues, as demonstrated when the periodicity of bioluminescence continued in the absence of prolonged darkness (Morse *et al.*, 1990). For dinoflagellates in near-surface waters, photosynthesis (autotrophs), as well as bioluminescence (both autotrophs and heterotrophs), is inhibited by high light, either by oxidation of luciferins (Lapointe and Morse, 2008) or



7.3 Depth distribution over time of bioluminescence potential (photons L^{-1}) measured with a UBAT bathyphotometer (Orrico *et al.*, 2009) from vertical profiler in San Luis Obispo Bay, CA between 7 and 14 April 2009. Profiles were taken every 30 min with a sampling rate of 2 Hz. The profiler is above water, so changes in depth reflect the tide height variation.

direct photodegradation of their photoproteins as is the case for ctenophores (Ward and Seliger, 1974). There is a lag time required for the molecules to be rebuilt and for cells/organisms to recover to exhibit their maximum bioluminescence potential (Lapota *et al.*, 1992a). Since dinoflagellates are often the dominant contributors to the overall light budget (Batchelder *et al.*, 1992; Lapota *et al.*, 1988, 1992b), these two factors have the largest influence over the periodicity observed in bioluminescence in the near-surface ocean. One additional factor that can be significant is the DVM from zooplankton. While there is a number of theories to explain this migration (see Williamson *et al.*, 2011), the net effect is an increased night-time abundance of zooplankton in the surface ocean. As a portion of the zooplankton community is bioluminescent, the net effect is an enhancement of the overall bioluminescence at night. The total impact of DVM on the light budget has been documented to range between 0% and 50%, with a mean of approximately 20% (Batchelder *et al.*, 1992; Lapota *et al.*, 1988, 1992a, 1992b).

An example of the combined effects of circadian rhythms, photo-inhibitory effects, and changes in community structure on the bioluminescence potential is illustrated in a 5-year study from 2005 to 2010 off the coast of California. Bioluminescence was repeatedly measured with a bathyphotometer (see Section 7.2) from a vertical profiler every 30 min at a sampling rate of 2 Hz. The data set represents over 100 million observations and is used here to quantify the mean *in situ* diel periodicity in bioluminescence at this



7.4 Diel variation in BP. Data were collected by the vertical profiler described in Fig. 7.3 from December 2005 until December 2010. For each day of data collection, data from the upper 2 m were scaled from 1 to 0 based on the daily maximum and minimum of bioluminescence. Each 30 min observation across the day was then normalized to the maximum and minimum mean values.

location, integrating not only the biological controls on bioluminescence, but the physical (i.e. upwelling, storm) dynamics in this coastal location. A representative week of data, showing the diel periodicity in bioluminescence, is shown in Fig. 7.3. Figure 7.4 shows this near symmetrical diel pattern in bioluminescence for the entire data set. These data have been integrated into efforts to dynamically model bioluminescence (see Section 7.3.3). The rapid transitions during dawn and dusk illustrate the need to consider these patterns when attempting to quantify bioluminescence in the near-surface ocean.

7.2 Measurement of bioluminescence in the ocean

‘...but it is a marvel that the liquid of this Pilmo when rubbed on black sticks and certain other things causes them to shine in darkness no differently than fire.’

Athanasius Kircher, 1664

A common feature across all bioluminescent organisms, with the exception of bioluminescent bacteria, is that mechanical stimulation leads to the emission of bioluminescence. The force required to mechanically stimulate organisms to emit light is about 1 dyne (10^{-5} N) cm^{-2} (Rohr *et al.*, 1998). When measuring bioluminescence there are generally two methods that have been

employed by the oceanographic community. The first is a method whereby a volume of water is agitated to stimulate bioluminescence, which is then measured with a photo multiplier tube (PMT). The second approach uses a low-light camera to either image the phenomena directly or to image a screen that is being moved through the water, stimulating organisms. Both techniques provide different quantifications of bioluminescence and both are important in understanding its distribution. In this section, we detail these two methods with some historical context, highlight the current methodologies in practice, and then detail results from these measurements with a description of the general distributions of bioluminescence in the ocean.

7.2.1 Open and closed systems

‘Fire sparkles from the water and the sailor imagines he is proceeding through a sea of fire.’

BuzurgibnShabriyar al-Ramhurmuzi, AD 953

Quantification of *in situ* bioluminescence in the marine environment began unexpectedly when attempting to measure the attenuation of solar radiation with depth with an upward looking photometer (Clark and Backus, 1956; Kampa and Bodin, 1953). As this photometer, which was fitted with a PMT, was lowered below the euphotic zone, it continued to record light pulses. In later work, the bioluminescence signal was isolated from the ambient light fields by simultaneous measurement of the incident radiation on the ocean surface (Clarke and Wertheim, 1956). This sensor, however, depended on the upward and downward motion of the profiler (and ship) and did not have either a constant stimulus for the organisms or a defined volume of measurement, limiting their abilities to quantify the light flux.

In order to overcome these limitations, as well as the interference of the ambient light fields on the bioluminescence measurements, Gittleson (1969) developed a semi-enclosed system that entrained water from the top of the instrument creating turbulence in front of a downward looking PMT. The uniformity of turbulence within the field of view relied on a constant ascent rate of the profiler. This design was modified with dual rotary fans (blades in opposite directions) on both the top and bottom of the detection cylinder (Levin *et al.*, 1977). The fans on the ends of the instrument created turbulence for stimulation of bioluminescence when the instrument was either raised or lowered. Because of the efficient baffling, this design is still being used to examine the vertical dynamics in bioluminescence over diurnal cycles (Utyushev *et al.*, 1999). These ‘open’ bathyphotometer designs were followed by the development of closed bathyphotometer systems that used pumping systems that created a defined the rate of flow through the detector chamber. This was motivated by the need to maintain consistent stimulation

of a known volume (Backus *et al.*, 1961; Clarke and Kelly, 1965; Seliger *et al.*, 1963). In addition, an ancillary motivation for the closed chamber design was to consider the flash intensities and duration of particular groups of bioluminescent organisms (Seliger *et al.*, 1969). This general design has been the basis for the suite of bathyphotometers presently in use, which has provided a qualitative understanding of the distribution and intensity of *in situ* mechanically-stimulated bioluminescence potential (BP). This is compared to the total stimuable light (TSL; *cf.* Buskey, 1992), which assays the complete BP of an organism via mechanical or chemical stimulation in a laboratory setting.

There has been much debate about the nature of the measurement and the accuracy of the suite of instruments that have been or are currently used to measure bioluminescence. One of the complications with the use of these bathyphotometers in quantifying BP has been that neither the residence times nor the hydrodynamic stimuli has been defined (Widder, 1997). Seliger *et al.* (1969) was the first to provide a theoretical basis for interpreting BP measured by bathyphotometers, by integrating the relationship between transit time through an instrument of known volume, for a population of known peak BP, and the exponential decay rate of that potential as:

$$L = K \int_0^T n V i_0 e^{-t/\tau} dt \quad [7.1]$$

where L is the total photons, K is the instrument calibration constant, n is the number of organisms per unit volume, V is the volume of the measuring chamber, i_0 is the initial flash intensity in photons per second, τ is the decay time constant of an exponentially decreasing flash (s), and T is the transit time of water through the chamber volume (s). After integration the equation reduces to:

$$L = K n V i_0 \tau \left(1 - e^{-T/\tau} \right) \quad [7.2]$$

T is dependent on both V and R , the flow rate of the instrument, i.e., $T = V/R$. The variables K , n , and i_0 can be held constant when comparing instruments. Therefore, according to this formulation, the measurement of BP is dependent on two primary factors: the transit time of a given volume, and the decay constant of the organism or community being measured. As Seliger *et al.* (1969) highlight, and Widder *et al.* (1993) re-examine, it is the ratio of T and τ that is critical. The ideal condition is when T is long relative to τ , and the entire flash occurs within the measurement chamber. If T is short relative to τ , the entire flash is not measured in the chamber and taken to its limit, $L \rightarrow 0$. Equation [7.1] can be rearranged and when $T \gg \tau$ then

$$L \cong KnVi_0 \tau \quad [7.3]$$

when $\tau \gg T$ then

$$L \cong KnVi_0 T \quad [7.4]$$

In these cases, the L can be divided by V to give a volumetric equivalence in units of photons per volume. When $T \gg \tau$, L/V is a constant value regardless of flow rate for a constant τ . However, in the case where $\tau \gg T$, the L/V value is a function of T and, thus, an inverse function of R since $V = TR$. Alternatively, using the $V = TR$ relationship, one could solve these equations in terms of L/T to give photons per unit transit time.

It is clear that there is a threshold of T/τ that is critical when making bioluminescence measurements in the environment. While the transit times of bathyphotometers can easily be defined, τ is a variable in the environment and dependent on the taxonomic composition of the bioluminescent community being measured. Table 7.1 provides a summary of past and existing bathyphotometers and the specifications defining their transit times. There are significant differences in the transit times, from 23 to 1400 ms. Given the ranges in τ from tens of milliseconds to seconds (*cf.* Herring, 1978; Latz *et al.*, 1987; Morin, 1983; Widder and Case, 1981), the threshold where T is greater than τ is therefore difficult to assess with the array of bathyphotometers in mixed populations. The High Intake Defined EXcitation (HIDEX) bathyphotometer was designed to quantify τ real time *in situ* for τ less than T (see Table 7.1) and shows that values of τ vary with depth and depend on the assemblage of bioluminescent organisms (Case *et al.*, 1993).

Lapota and Losee (1984) showed that as the intensity of the flash and the duration of the flash increases, the rise time to the maximum flash is longer when comparing dinoflagellates to planktonic invertebrates. Using these data, τ was estimated for two dinoflagellates (*Ceratiumbreve* and *Ceratiumhorridum*), four copepods (*Centropagesfurcatus*, *Paracalanusindicus*, *Corycaeus speciosus* and *Corycaeus latus*) and two euphausiids (*Euphausiaeximia* and *Nyctiphanes simplex*). The mean values of τ were within the range of previous studies (Seliger *et al.*, 1969) and ranged from 60 ms for the dinoflagellates to 724 ms for the euphausiids, with the copepods averaging 243 ms. These values of τ are used here in combination with the bathyphotometer transit times (Table 7.1) to assess the variability in the measurement of BP relative to the bioluminescent organism. For dinoflagellates with rapid flash decay constants, the majority of the bathyphotometers have transit times that are sufficiently long to measure the entire flash (Fig. 7.5a). As the decay constant increases, the amount of standardized bioluminescence intensity measured by the BPs is less uniform and is different

Table 7.1 Comparison between volume (V), flow rate (R), transit time (T), sampling frequency and method of mechanical stimulation of the past and present bathyphotometers

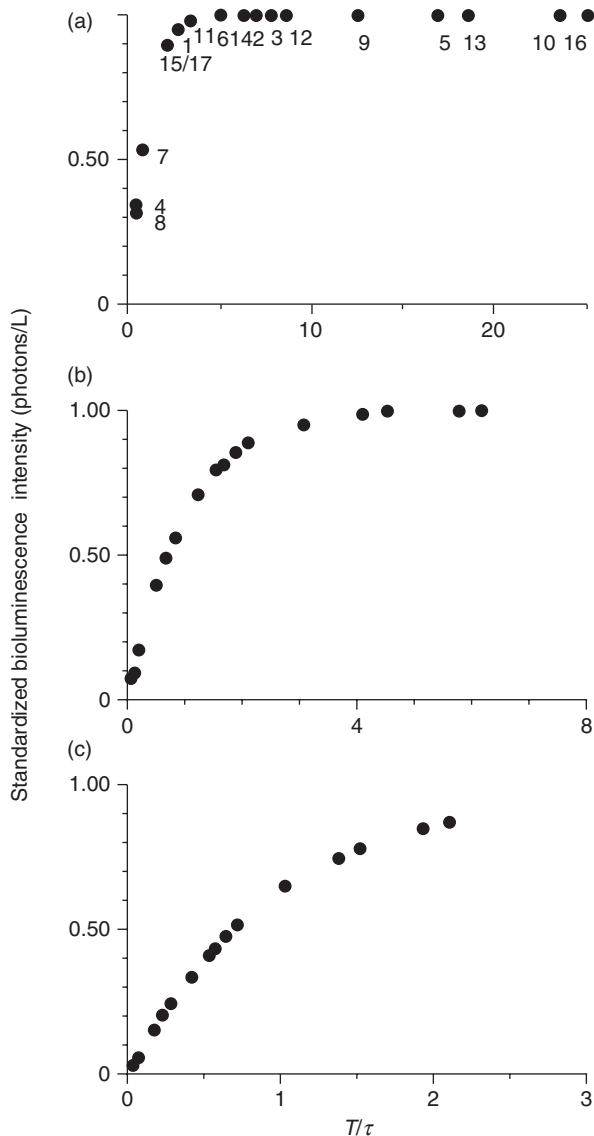
#	Inst. Name	V (L)	R (Ls^{-1})	T (s)	Freq. (Hz)	Stimulation	Reference
1	Deep-sea	0.06	0.37	0.16	?	Impeller	Clarke and Kelly, 1965
2	Towable	0.045	0.11 ^a	0.41	10	Impeller	Seliger <i>et al.</i> , 1969
3	U.S. Navy	0.051	0.11	0.46	2	Impeller	Soli, 1966
4	Deep-sea	0.038	1.5	0.025	?	Impeller	Aiken and Kelley, 1984
5	ML 83-89	0.3	0.3	1	96	Blunt body	Swift <i>et al.</i> , 1995
6	ML 91	0.018	0.06	0.3	96	Blunt body	Swift <i>et al.</i> , 1995
7	Biolight	0.026	0.56	0.046	1-10 ⁵	Constriction	Losee <i>et al.</i> , 1985
8	Profiling	0.026	1.1	0.023	1-10 ⁵	Constriction	Losee <i>et al.</i> , 1985
9	UTHIDEX	4.7	6.3	0.746	1000	Grid	Buskey, 1992
10	ML 87-88	0.3	0.214	1.4	96	Blunt body	Balchelder <i>et al.</i> , 1990
11	APL-BP	0.2	1	0.2	?	Undefined	Nelson, 1985
12	HIDEX	11.3	16-44	0.513 ^b	500	Grid	Case <i>et al.</i> , 1993
13	MDBBP	0.5	0.45	1.1	2	Impeller	Herren <i>et al.</i> , 2005
14	ÉcoleNavale	0.19	0.5	0.38	0.25-0.5	Grid	Geistdoerfer and Vincendeau, 1999
15	GLOWtracka	0.012	0.1	0.123	50	Grid	Kim <i>et al.</i> , 2006
16	UBAT	0.44	0.3	1.467	60	Impeller	Orrico <i>et al.</i> , 2010
17 ^c	XBP	1.96	15.71	0.124 ^d	>3	Grid	Fucile, 1996; Fucile <i>et al.</i> , 2001

^a Flow for optimal sensitivity (Seliger *et al.*, 1969).

^b Based on optimal stimulation at 22 Ls^{-1} (Widder *et al.*, 1993).

^c This is not a bathyphotometer, but a free-falling instrument included for comparative purposes.

^d Based on a drop speed of 2.7 ms^{-1} and estimate of flow (Fucile, personal communication, 5 June 2005).



7.5 Standardized bioluminescence intensity (photons L^{-1}) as a function of the ratio of the transit time of water through the chamber volume (T ; s) and the decay time constant of an exponentially decreasing flash (τ ; s). The three panels represent the simulated performance of current and past bathyphotometers (numbers correspond to bathyphotometers listed in Table 7.1) assuming equivalent stimulation of BP. Given T is a fixed parameter for each bathyphotometer, the panels represent the performance with organisms of increasing values of τ ; 60 ms to simulate dinoflagellates in (a), 243 ms for copepods in (b) and 724 ms in (c) to simulate longer flashing euphausiids. As the flash time increases, the measured BP signal in the bathyphotometers decreases. As T is a fixed parameter, the order of each bathyphotometer is the same for each panel.

in every instrument (Fig. 7.5b and 7.5c). Some standardization between those instruments on the linear portion of the slope in Fig. 7.5b and 7.5c could be accomplished by dividing the L/V values by the transit time, T (the linear portion of the slope is the region where τ is sufficiently larger than T to satisfy the numerical conditions of Equation [7.4]). However, in the region of these curves where the slope is changing, L/V is a non-linear function of T and for a given sample, each instrument will yield a different L/V and $L/(VT)$ value. These differences are solely based on variations in chamber volume and flow rate, illustrating that absolute quantification of *in situ* BP of higher trophic level organisms, known to contribute significantly to near-surface bioluminescence remains a challenge.

In addition to the variables formulated by Seliger *et al.* (1969) and Widder *et al.* (1993) has detailed a number of other considerations when measuring BP. The size of the intake relative to the flow rate was a specific consideration when designing the HIDEEX BP to ensure capture of larger bioluminescent organisms. The size of the inlet diameters (some as small as 1.3 cm) of these instruments raises concern over what the instrument may be actually capturing. In a recent study assessing bathyphotometer capture efficiency, there was no significant difference between the planktonic community caught by the bathyphotometer (with an inlet diameter of ~4 cm, Number 13 in Table 7.1) from that in the water column (Herren, 2005). Defining the hydrodynamic stimulation of a bathyphotometer has also been shown to be important (Widder *et al.*, 1993). While bathyphotometers that have variable flow rates can maximize hydrodynamic stimulation by increasing the flow rate, this will be at the expense of increasing the transit time and possibly impacting the abilities to capture the entire flash decay. Another consideration is the sampling frequency of the instrument. If the frequency of the sampling is higher than transit time, as is the case for almost all designs (Table 7.1), then averaging the signal makes it possible to assess the total light generated from a given volume. If, however, the sampling frequency is lower than the transit time, as for (Geistdoerfer and Vincendeau, 1999), then a portion of the signal is missed and defining small-scale features in the environment is not possible. Given all of these considerations, measurements of *in situ* BP will vary between bathyphotometers as a function of the assemblage of organisms captured, the transit time, and the level of hydrodynamic stimulation. Comparisons between measurements of BP and TSL indicate that the overall efficiencies of the instruments are comparable and range between 10% and 20% (Batchelder and Swift, 1988; Case *et al.*, 1993; Herren *et al.*, 2005). Although many organisms contribute to the BP in surface waters over broad temporal and spatial scales (Lapota and Losee, 1984), dinoflagellates and copepods have been found to dominate the majority of the bioluminescence in the world's oceans. These smaller organisms have relatively shorter values of τ and do not have the intake avoidance potential

of larger organisms; thus the bathyphotometers presently being used in the field appear to provide sufficient *in situ* BP measurements necessary for understanding bioluminescence distributions in the ocean.

7.2.2 Imaging approaches

‘In the same way, the glitter of the sea, of fish and putrid wood depends on motion.’

Domenico Bottoni, 1692

While bioluminescence has been witnessed for millennia, the ability to capture ‘images’ of the phenomenon was restricted to verbal descriptions and through painting (Beebe *et al.*, 1934) until the mid 1960s. The first images of bioluminescence were generated with the development of image intensifying systems applied to bioluminescent organisms in the laboratory (Eckert and Reynolds, 1967; Reynolds, 1964). Since then, imaging systems have been used to document the sub-cellular structure of light-producing organelles (Widder and Case, 1981) and distributions of light organs on a variety of species (Widder, 2002). Bioluminescence imaging has also transitioned into the ocean and is a current tool for quantifying oceanic distributions of bioluminescent organisms. Knowing the limitations of imaging passive bioluminescence, Widder *et al.* (1989) developed an intensified camera system on a submersible that would view screen mesh travel through the water. This system allowed for a number of novel discoveries, including a new appreciation of the number gelatinous species (often destroyed in traditional net tows), quantification of bioluminescent sources, and light production. Eventually, the system was also able to generate the 3-dimensional distributions of organisms *in situ* (Widder and Johnsen, 2000) and elucidated understanding of the thin layering of organisms in the ocean (Widder *et al.*, 1999). This same basic technique has been applied to a lander outfitted with an imager and horizontal screen (Priede *et al.*, 2006). The lander is dropped from a ship and free-falls to depths of over 4000 m, and has been used to evaluate vertical differences in bioluminescence as well as seasonal changes (Gillibrand *et al.*, 2007a). The same lander system also has a direct imaging system that is able to record *in situ* bioluminescence events on the seafloor, either baited or unbaited. These studies have shown the heterogeneous distribution of bioluminescence on the seafloor (Gillibrand *et al.*, 2007b) and suggest that bioluminescent queues might be more important in location of food sources and habitat colonization than previously thought (Craig *et al.*, 2011). Another example of direct imaging of bioluminescence *in situ* comes from work of Morin and Cohen (1991, 2010) documenting the vertical displays of male ostracods in courtship displays. Imaging above the surface of the ocean with a low-light detector, called the Stabilization Airborne Night Observation System (SANOS), has also been used to detect and map the

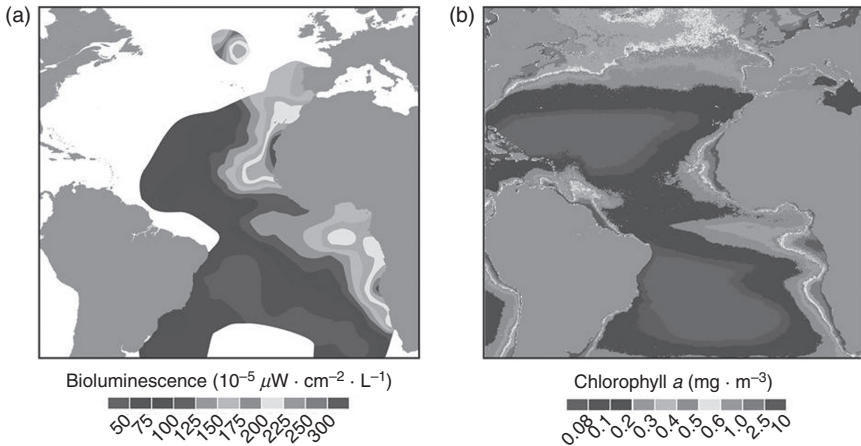
distributions of bioluminescence associated with schools of Spanish mackerel off the coast of Florida as a management tool (Roithmayr, 1970). Miller *et al.* (2005) also demonstrated how to use a low-light Operational Linescan System on board a Defense Meteorological Satellite Program satellite to image a surface slick of bioluminescent bacteria extending over 15 000 km² in the Indian Ocean.

7.2.3 Distribution of bioluminescence in the ocean

'It is not only when the sea is agitated that it becomes brilliant but we have seen more [lights] toward the equator during the calm after the sun sets.'

Pere Guy Tachard, 1685

Morin (1983) has documented that approximately 1–3% of the biomass in the surface ocean belongs to bioluminescent taxa. While there is large variability in this proportion, depending on location and time of year, one would expect the distribution of bioluminescence to mimic biomass distributions (Lapota, 1998). A recent review highlighting bioluminescence distributions shows to first order that this general assumption is met at a range of scales from biological thin layers to ocean basins (Haddock *et al.*, 2010). For the few data available at the basin scale, surface oceanic distributions of bioluminescence distributions reveal the large-scale circulation patterns (i.e. the Atlantic gyres and upwelling features off the coast of Africa), which govern nutrient availability and structure the biological community, as seen in the correspondence with chlorophyll *a* distributions (Fig. 7.6). At this scale, the spatial and temporal overlap between bioluminescent autotrophs and heterotrophs is relatively uniform; however, as the scales decrease, these groups become more distinct. At the regional scale, bioluminescence can be prominent at various times of the year from successions of blooming species. These can be almost exclusively autotrophic (Lapota, 1998; Swift *et al.*, 1995), heterotrophic (Moline *et al.*, 2009; Swift *et al.*, 1985), or a mixture, usually later in the bloom cycle (Geistdoerfer and Cussatlegras, 2001; Lapota, 1998; Lieberman *et al.*, 1987). In temperate (Blackwell *et al.*, 2008) and polar (Buskey, 1992; Lapota *et al.*, 1988) regions, the total light produced follows a seasonal biomass cycle; however, bioluminescence is present year-round (Berge *et al.*, 2012; Lapota, 1998; Nealson *et al.*, 1984). In tropical regions, where autotrophic biomass is often nutrient limited, there is lower bioluminescence intensity from a less abundant but more diverse community (Vinogradov *et al.*, 1970). On a small scale, as in the case of biological thin layers, organized meter-scale vertical layering is often species-specific and bioluminescence can be either associated or absent within these layers (Benoit-Bird *et al.*, 2010; Moline *et al.*, 2010). These differences in community structure, and thus bioluminescence, at small time and space scales have made it difficult to relate other environmental variables or processes



76 Oceanic-scale distributions of (a) bioluminescence and (b) chlorophyll *a* in the Atlantic. The distribution of bioluminescence is drawn from data in Piontkovski *et al.* (1997) and represents a 20-year data set of the mean bioluminescence from 0 to 100 m. The satellite retrieval represents the mean field of chlorophyll *a* from the combined SeaWiFS and MODIS-Aqua ocean color sensors for the period between September 1997 and February 2009. Data for the chlorophyll map in (b) were retrieved from the Giovanni online data system, developed and maintained by the NASA Goddard Earth Sciences (GES) Data and Information Services Center (DISC). (Source: Redrawn from Haddock *et al.* (2010) with permission from the authors.)

to bioluminescence in a predictive manner (Marra *et al.*, 1995; Ondercin *et al.*, 1995). Recent work, however, has used the difference in flash intensity between groups to delineate autotrophic from heterotrophic bioluminescent organisms to reveal their interactions (Moline *et al.*, 2009). While most studies examining the distribution of bioluminescence have been focused on the near-surface ocean, vertical profiles of deep-sea bioluminescence have been collected using free-falling landers (Preide *et al.*, 2006). These distributions show an exponentially decreasing signal with seasonal deep maxima (Gillibrand *et al.*, 2007a), indicative of classical particulate carbon profiles (Menzel, 1967) and the seasonal pulse of surface material to the deep ocean.

7.3 Propagation of bioluminescence in and out of the ocean

‘At the stern of the ship where the water is cut through, you see at night, very deep under water, bubbles rise and break, then this shining or lustre is not there.’

Fredrick Martens, 1761

Propagation of bioluminescence in and out of the ocean began largely as a theoretical exercise, independent from the ongoing measurements of bioluminescence in the field. Gordon was a pioneer in this area, first examining the feasibility of detection on bioluminescence from space and the dependence on in-water scalar irradiance (Gordon, 1984). The work continued (Gordon, 1987), gathering all the recent relevant data sets (Bricaud *et al.*, 1983; Morel and Prieur, 1977; Petzold, 1972; Smith and Baker, 1978) to make an estimation of irradiance at the sea surface from a point source of light. He quickly established that the propagation of light only relied on the independent influences of absorption and the scattering phase function and developed an analytical solution and Monte Carlo simulation for an oligotrophic ocean case where phytoplankton was the only optical constituent in addition to water. He concluded that for shallow source depths, the attenuation of light approximated absorption (a) and backscattering (b_b) and that the attenuation coefficient could be approximated at night by this method. Gordon (1987) was part of larger programs (Biowatt and Marine Light-Mixed Layer [MLML]; Marra, 1984; Marra and Hartwig, 1984; Marra *et al.*, 1995), which were the first large-scale attempts to relate physical oceanography to the optical (including bioluminescence) variability of the water column (Marra, 1984). Biowatt and MLML were also some of the first programs to recognize the importance of an accurate description of the optical properties of the water column in both of the propagation of light and the ecological structure (Carder *et al.*, 1995; Dickey *et al.*, 1993; Odercin *et al.*, 1995; Smith *et al.*, 1989; Stramska *et al.*, 1995). A photon budget (sources and sinks) for the North Atlantic area studied in these programs was constructed, which included bioluminescence (Smith *et al.*, 1989). While important in evaluating the influence of major optical constituents on biological processes, bioluminescence was not a focus and, in the context of photon budgets, this work concluded the obvious – that bioluminescence became more important with depth and was 5–9 orders of magnitude less important than other processes in the surface ocean. It was also mentioned that there was no attempt to propagate bioluminescent photons out of the surface as part of the budget.

Yi *et al.* (1992) tried to expand on work by Gordon (1987) for conditions with heterogeneous bioluminescence source distributions with consideration of ambient light (i.e. moonlight) by the combined measures of irradiance and scalar irradiance at two depths. This work was solely theoretical and did not test the approach with field measurement. The integration of in-water optical properties and bioluminescence has been absent in the literature until only recently, when two focused studies examined the propagation of bioluminescence (Moline *et al.*, 2007; Oliver *et al.*, 2007; Orrico *et al.*, 2013). This section will highlight these two studies as case examples, followed by recent efforts to integrate bioluminescence into hydrodynamic modeling. The

section and review will conclude on future directions for the study of oceanic bioluminescence.

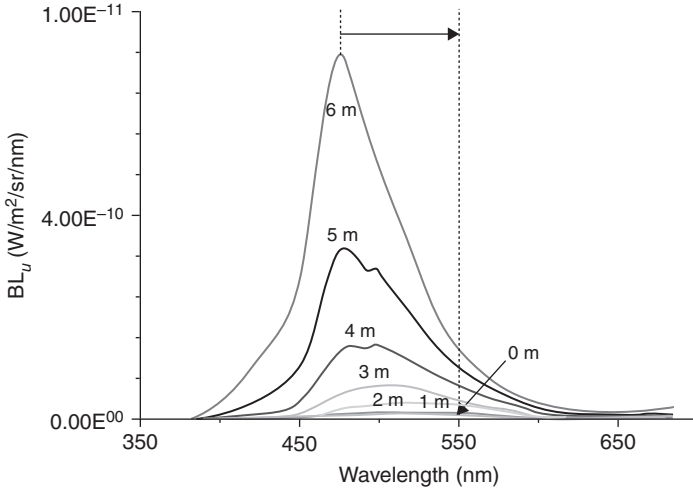
7.3.1 Case study 1: radiative transfer modeling

‘The vessel drove before her bows two billows of liquid phosphorus, and in her wake she was followed by a milky train.’

Charles Darwin, 1839

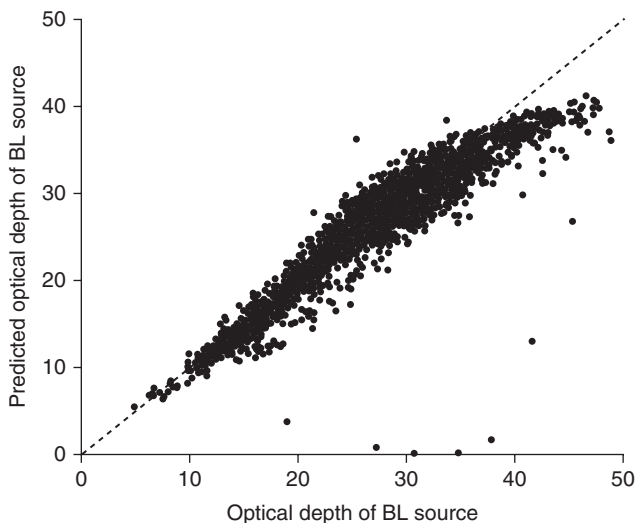
There have been significant advances in the development of optical sensors during the same period of bathyphotometer development. This development has been fueled, in part, by the need for in-water validation of ocean color satellites, as well as the Naval need to define the inherent optical properties (IOP) for visibility and performance prediction modeling (Dickey and Chang, 2001; de Rada *et al.*, 2009). The most significant advances in optical instrumentation have been the development of sensors that can directly measure *in situ* IOPs, such as the Wetlabs Inc. AC-9 and AC-S for the measure of spectral absorption and attenuation, the ECO-VSF for estimates of the volume scattering function, and single wavelength/angle backscatter sensors. These measurements are critical for reasonable quantification of bioluminescence propagation and of bioluminescence water-leaving radiance (BL_w) in coastal regions (Gordon, 1987). The development of compact off-the-shelf (COTS) optical sensors and bathyphotometers (Table 7.1) also provides an opportunity even small research groups to combine the *in situ* measurements of BP and IOPs for development/advancement of techniques for simultaneous estimates of BL_w . In addition to COTS sensor development, there has been a concerted effort to develop user-friendly radiative transfer modeling programs (i.e. HydroLight, Sequoia Scientific Inc., Bellevue, WA) for use by the general science community (Mobley, 1994).

Here we highlight a study that combined measurements from optical sensors, a bathyphotometer, and a radiative transfer model to estimate BL_w from a defined source. This was a two-part study: the first part was to propagate light from the stimulated source through the ocean surface (Moline *et al.*, 2007); the second part was to use a neural network model trained on a portion of the data to predict the source depth solely from the leaving radiance (Oliver *et al.*, 2007). Briefly, simultaneous vertical profiles of BP (#13 in Table 7.1) and spectral IOPs were collected every 20–30 min from an autonomous profiling system over two summer periods to examine temporal changes in bioluminescence potential and optical signatures in relation to the highly dynamic physical regime. These measurements were then integrated into the new bioluminescence module of HydroLight with modifications to distribute internally generated plane parallel photons to yield an estimate of BL_w (see Stephany *et al.*, 2000). The goal of this work was to estimate BL_w at the surface for each meter of the water column (assuming



7.7 Example of the spectral shift in the maximum wavelength of the upward bioluminescence radiance (BL_u) at meter intervals away from the source predicted by from Hydrolight based on stimulation of bioluminescence at 7 m. This example was for one depth for one of the 48 daily profiles of the 23 day study (Moline *et al.*, 2007). Simulation used measured BP, spectral scattering, spectral absorption, and backscatter at each meter depth interval.

each meter was stimulated independently). Profiles of BP were spectrally reconstructed using known spectra from a range of dinoflagellate and copepods bioluminescence emission spectra (Fig. 7.2). Thirty-six wavelengths of BP from measurements within each meter were then propagated through the surface waters using measured values of spectral absorption, attenuation, backscattering, and sea state conditions as inputs into HydroLight. The BL_w results provided a qualitative picture of the significant variability in the BL_w even over a single night, highlighting the need for continuous simultaneous measurements of BP and IOPs when estimating BL_w (Moline *et al.*, 2007). An example of the propagation of bioluminescence radiance (BL_u) from this procedure from one of the meter intervals is shown in Fig. 7.7. As with the spectral shift in solar radiation with depth, BL_u showed a significant shift of over 80 nm from blue to green as light propagated to the surface and a 40-fold decrease in the relative contribution of blue wavelengths with BP stimulated at depth (Fig. 7.7). The significant spectral shift in propagated bioluminescence suggested that this could be a variable to invert the problem and, with an above-water sensor with adequate sensitivity and spectral range (Lynch, 1981), may be able to predict the geometric depth of the source. In order for results in this study to be universally applicable, the relationship between spectral peak of BL_w , BL_w itself, and the optical depth (not geometric depth) was established (Moline *et al.*, 2007). Half the data



7.8 Measured versus modeled predicted source depths (optical depths) of BP from BL_w . Neural nets were trained on BL_w and their associated optical depth from year 2000, and they were then used to predict the optical depth of the bioluminescent layers in year 2001. The RMS error was small compared to the range over which the neural net was asked to predict. Dashed line is the 1:1 line.

from the field study (the first year) were incorporated into a neural network model as a training data set to then predict the source depth from only BL_w (Oliver *et al.*, 2007). The results showed a significantly robust ability to predict the source depth from the spectral shift (Fig. 7.8). The prediction was also challenged by varying the IOP inputs two orders of magnitude and adding various reflective bottoms to simulate a wide range of environmental conditions (optical depths ranged from 0.1 to 55), and still found to be robust (Oliver *et al.*, 2007). As the ability to predict the bioluminescence source depth was inherent to the spectral shift in BL_w , a data denial experiment was used to examine the number of wavelengths required to maintain the robust BP source depth prediction. From the initial 36 wavelengths used, it was found that as little as three wavelengths (380, 492.5 and 645 nm) from the spectrum of BL_w were sufficient for an accurate determination of the depth of the bioluminescent source (Oliver *et al.*, 2007).

7.3.2 Case study 2: empirical point source modeling

‘I have extracted from the sea glittering seaweed and, by throwing in some linen which becomes tinged with splendor, I have communicated light to neighboring things, emulating the stars.’

Thomas Bartholin, 1647

A bioluminescent organism, and population of bioluminescent organisms, can be considered to be an isotropic light source emitting radiant spectral power ($\text{W m}^{-3} \text{nm}^{-1}$) into 4π sr. In a volume of water, the intensity of bioluminescence can be considered to be the sum of the light emitted from all the point sources for a known time period. As demonstrated by Gordon (1987) analytically, induced bioluminescence is attenuated as it propagates to the surface and is lost due to absorption or backward scattering. However, forward scattered light is not lost and can be detected. In the context of this work, here we consider and test three models to describe the attenuation of bioluminescence as it propagates to the surface. This was part of a larger bioluminescence detection experiment described in Orrico *et al.* (submitted). The first model is the equation for irradiance attenuation, where attenuation coefficient (K) describes the near-exponential decrease in irradiance as it propagates to the surface. K can be approximated by measuring the forward scattering from a collimated point source and diffuse detector that has an acceptance angle close to 180° (Jerlov, 1976). Thus, the attenuation of bioluminescence can be described as:

$$E_{\text{BL}}(0^+) = E_{\text{BL}}(z) \cdot (a + b_z)^{*z} \quad [7.5]$$

where $E_{\text{BL}}(0^+)$ is the bioluminescence irradiance at the surface, $E_{\text{BL}}(z)$ is the intensity of induced bioluminescence at depth, z . However, this situation refers to the attenuation of daylight in a plane parallel situation and this is not the case for bioluminescence, which occurs only at night.

Another possible equation to describe the attenuation of bioluminescence is to measure the forward scattered light of a collimated point source and detector with an acceptance angle close to 0° . Here, the attenuation coefficient is approximated by the beam attenuation coefficient $K = c$. Thus, Equation [7.5] can be re-written as:

$$E_{\text{BL}}(0^+) = E_{\text{BL}}(z) \cdot e^{-cz} \quad [7.6]$$

The diver visibility model, as formulated in Equation [7.6], describes the attenuation of natural light spectrum convolved with the spectral responsivity of the human eye (Zaneveld and Pegau, 2003). In this case, visibility of a black target depends on the beam attenuation coefficient, measured at 532 nm. However, this theory pertains only to the underwater visibility of a submerged target in the horizontal direction with ample ambient light, and does not deal with the transmission through the surface. The situation with bioluminescence detection is clearly different as vertically propagated light is being investigated.

Gordon (1987) analyzed the distribution of radiance at the sea surface due to an embedded point source and showed that there is an attenuation

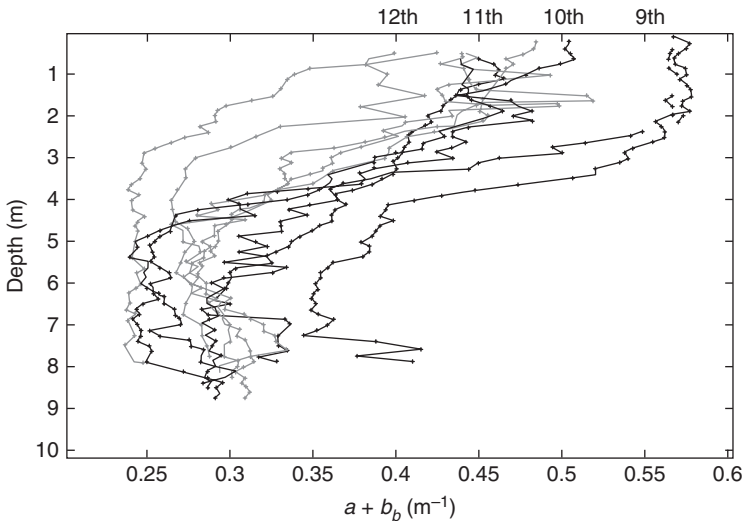
coefficient, k ($k \approx a + b_b$), associated with the point source that describes its attenuation in addition to the spherical spreading. This result was also obtained by measurement (Maffione *et al.*, 1993). Thus, to determine the intensity of bioluminescence irradiance at the surface, E_{BL} (photons $m^{-2} s^{-1}$) measured at the source is propagated to the surface by solving the following:

$$E_{BL}(0+) = \left(E_{BL}(z) \frac{1}{z^2} \right)^{-(a+b_b)gz} \quad [7.7]$$

where $K = a + b_b$ as it does with the daytime attenuation, but the $1/z^2$ term is added to account for the rate of light lost due to spreading of a point source. Since bioluminescence has been shown to shift into the green as it propagates to the surface (Moline *et al.*, 2007), especially in coastal environments, the attenuation coefficient ($a + b_b$) is optimally measured at 500 nm.

Work was conducted over a 4 day period (9–12 August 2010) off the Center of Coastal Marine Science pier in San Luis Obispo Bay, CA, where the maximum depth is approximately 12 m. The pier is located in a region where ambient light from nearby coastal communities of Port San Luis, Avila Beach, Pismo Beach, and Oceano is minimal. This period was chosen because of the new moon phase and based on routinely high bioluminescence during this period (even though not used directly here). A vertically profiling cage was used to measure the vertical structure of the water column optical properties. A reflecting tube absorption meter (AC-S) with no scattering correction was used to approximate $K \approx a + b_b$ at 500 nm, where the meter provides $a + b_b$ nearly exactly (Moore *et al.*, 1992; Zaneveld *et al.*, 1994). To verify the most appropriate model to describe bioluminescence attenuation, it was important to have a consistent isotropic light source. Here, a blue light source (Glo-Toob™) was mounted to the bottom of the profiling cage and measured by an open-faced PMT detector as it was profiled below the cage (fixed at the surface) from 0.75 to 11 m. With the diffuser adaptor attached, the Glo-Toob™ provided a constant near-isotropic light source with a spectral output peak of 465 nm, and was a good approximation of bioluminescence (Fig. 7.2). E_{BL} was modeled as a function of three possible models described in Equations [7.5], [7.6], and [7.7]. Constant $a + b_b$ and c were used as model inputs for all three models (mean value at 2 m). In addition, Equation [7.7] was also solved for $a + b_b$ that varied vertically with depth.

In general, water column optical properties were vertically stratified during the period of the experiment. Maximum values of $a + b_b$ at 500 nm were found from the surface to 2 m and decreased with depth (Fig. 7.9). During the period of the experiment, the water column became increasingly more transparent in this wavelength over time. Mean values in the surface were greatest on 9 August 2010 ($0.58 m^{-1}$) and decreased to a minimum on



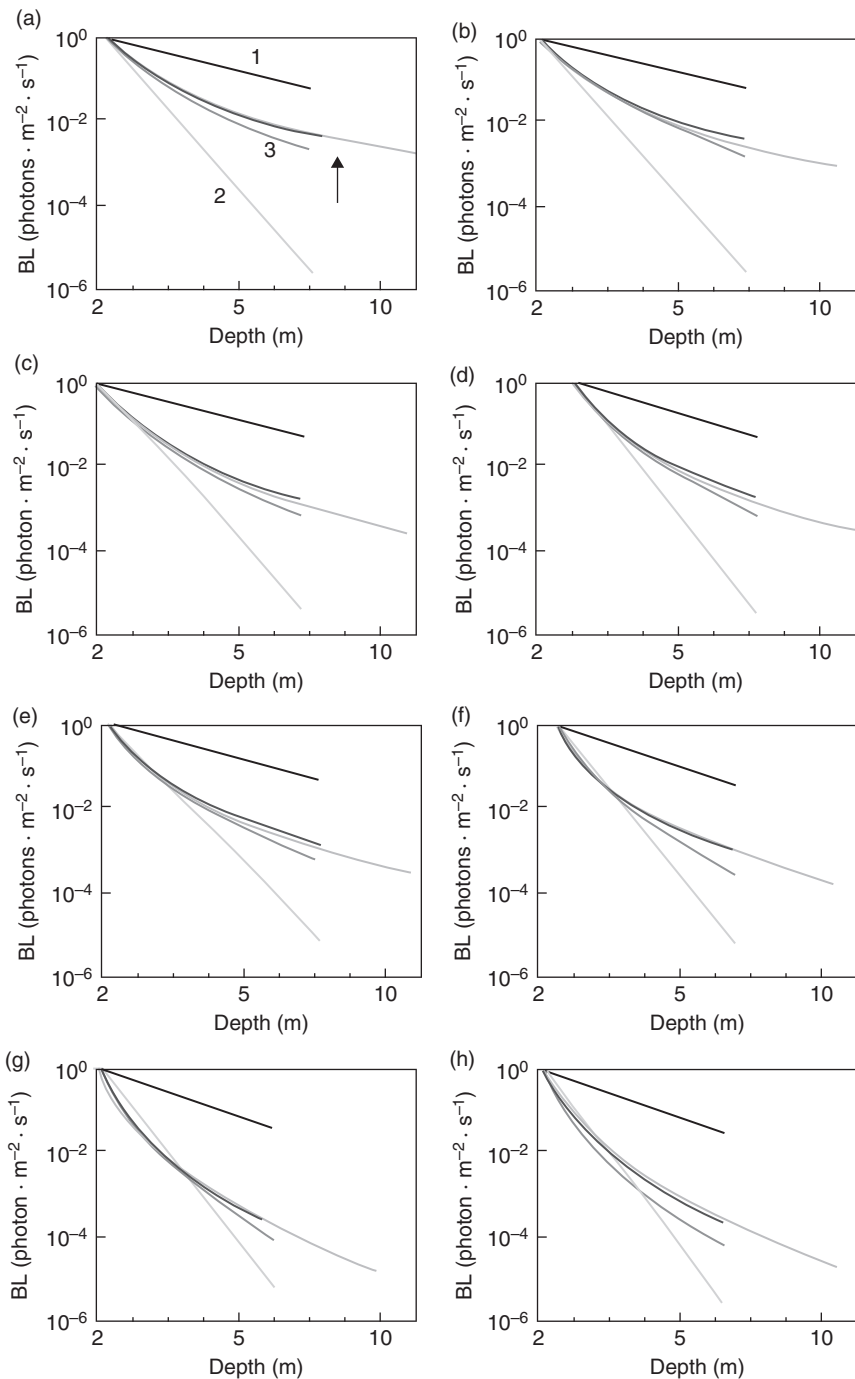
7.9 Vertical structure of $a + b_b$ (absorption a , and backscatter coefficient b_b) at 501 nm, measured from the 9th through the 12th of August 2010 in San Luis Obispo Bay. Duplicate profiles were made for each day indicated by the data. There was a transition to more transparent water as the experiment progressed.

12 August 2010 (0.37 m^{-1}). The light source was lowered twice each night period, before and after additional experiments not detailed here (Orrico *et al.*, 2013), to evaluate changes in the attenuation of the blue source. The fit of the measured point source attenuation to attenuation models Equations [7.5], [7.6], and [7.7] is shown for each profile (Fig. 7.10). For all models both mean (constant) $a + b_b$ or c values at 2 m were used for model input. However, for Equation [7.7] depth variation in $a + b_b$ was also used to reflect any changes in model performance. As hypothesized by Gordon (1987), the intensity of a blue point source at the water surface was best modeled by Equation [7.7], where $a + b_b$ measured at 500 nm describes the attenuation of blue light as it propagates to the surface (Fig. 7.10). This was true when using mean values of $a + b_b$ (at 2 m) or when taking the depth variability of $a + b_b$ into consideration; however, the model fit improved considerably with knowledge of the depth variability in a and b_b (Fig. 7.10).

7.3.3 Ecological modeling

‘...how in some places the sea is wont to shine in the night as far as the eye can reach; at other times and places, only when the waves dash against the vessel ... whereas in other seas the observation holds not...’

Robert Boyle, 1681



7.10 Comparison of measured point source attenuation of a Glo-ToobTM (arrow), to four modeled attenuations as a function of profile depth. Equations [7.1] and [7.3] were calculated constant $a + b_b$.

There is a strong emphasis by the oceanographic community to integrate ecosystem dynamics into hydrodynamic models (see Allen *et al.*, 2010). This is motivated by the need to improve understanding of biogeochemical cycles, natural resource availability, and climate cycles. Although there is a large diversity of models, most have some level of compartmentalization of biological groups based on trophic status, nutrients dependent on form and processes, and physical interactions, such as hydrodynamic and light field for driving primary production (see Doney *et al.*, 2009). To date, only a few modeling efforts have incorporated bioluminescence (Shulman *et al.*, 2003, 2005, 2011a, 2011b), taking advantage of another biological measurement (in addition to chlorophyll *a*) to potentially delineate trophic groups (Moline *et al.*, 2009). These studies have been focused on evaluating the short-term advection of bioluminescence in the coastal ocean, as the physical models are best able to reproduce local circulation structure using data assimilation techniques to initialize and constrain their solutions (Haidvogel *et al.*, 2000). As the need for higher resolution increases, as the complexity increases towards the coast, the number of observations required for assimilation also increases. This observational constraint effectively limits the time window that is effectively modeled, in this case, 1–3 days if only based on single set of observations.

Reasonable estimates of advection and diffusion from a physical simulation would allow one to describe an advection–diffusion equation for the bioluminescent particles:

$$\frac{\partial C}{\partial t} = -u \frac{\partial C}{\partial x} - v \frac{\partial C}{\partial y} - w \frac{\partial C}{\partial z} + \frac{\partial}{\partial x} \left(A^h \frac{\partial C}{\partial x} \right) + \frac{\partial}{\partial y} \left(A^h \frac{\partial C}{\partial y} \right) + \frac{\partial}{\partial z} \left(K^h \frac{\partial C}{\partial z} \right) + S(x, y, z, t) \quad [7.8]$$

where C is the concentration of bioluminescent particles, A^h and K^h are horizontal and vertical diffusivities, (u, v, w) are components of fluid velocity taken from the hydrodynamic model, and $S(x, y, z, t)$ is the source minus sink term for C . The first three terms describe the advection of C in the horizontal and vertical directions, the next three terms describe the diffusion of the particles, and the last term is the non-physical sources and sink term.

7.10 Continued

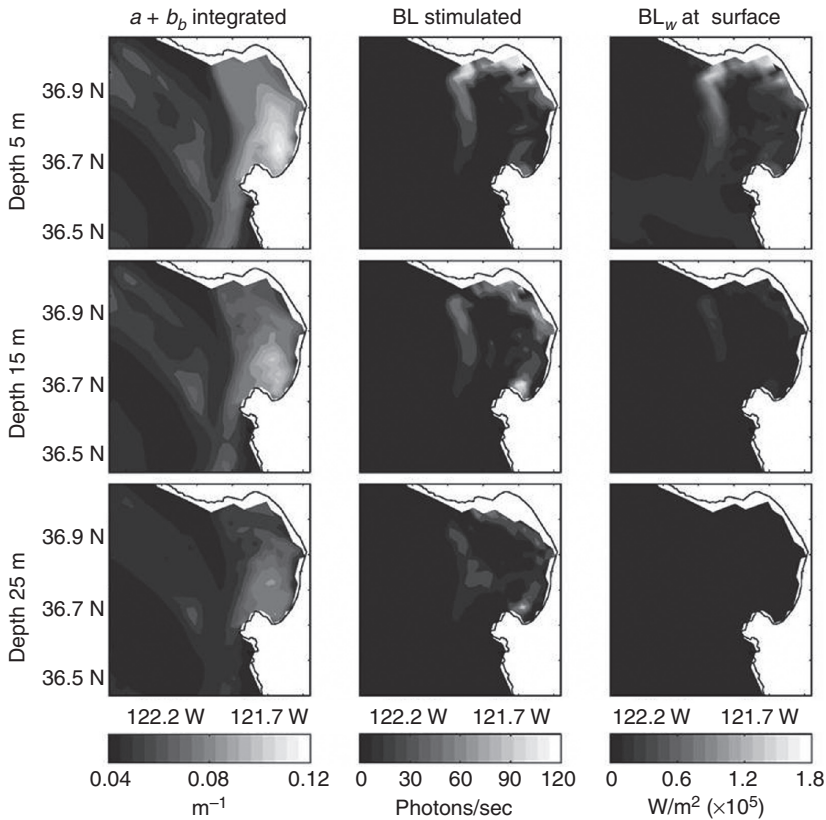
Equation [7.2] was calculated with constant attenuation. The modeled line above Equation [7.3] in (a) is same as Equation [7.3] but calculated with depth varying $a + b_b$ (see text for full description of equations). Duplicated comparisons were made on each of four nights from the 9th (a and b) through the 12th (g and f) of August 2010 in San Luis Obispo Bay. Measurements of absorption, a , and backscatter coefficient, b_b , are from Fig. 7.9.

Equation [7.8] represents the advection–diffusion–reaction (ADR) model. By initializing a validated physical forecast model with a realistic nowcast of the distribution of bioluminescent particles, one could develop an estimate of the future distribution of these particles strictly based on physical processes. For initialization, available BP observations are assimilated into the above ADR model by using the source term $S(x,y,z,t)$ in the following form (Shulman *et al.*, 2003, 2005):

$$S(x, y, z, t) = \gamma(C - C^0)\delta(\tau - \tau^0), \quad [7.9]$$

where C^0 are BL observations, γ is the scalar nudging coefficient multiplying $(C - C^0)$, τ is the location in the model domain with coordinates (x,y,z) , τ^0 is the location of the observed BL (C^0) with coordinates (x^0,y^0,z^0) , and $\delta(\tau - \tau^0)$ is a Dirac function for which $\delta = 1$ when $\tau = \tau^0$ and $\delta = 0$ for all other cases. Velocities and diffusivities in Equation [7.8] are taken from the initialization day and kept unchanged during the initialization–assimilation procedure. In this case, the assimilated BP (concentration C) is spread throughout the model domain until equilibrium is reached (when the value of $\partial C / \partial t$ is zero in Equation [7.8]). This provides the initial BP distribution, which is dynamically balanced with the physical conditions at the time of the initialization (see Shulman *et al.*, 2003, 2005 for more details). The equilibrium field C is used as the initial tracer distribution for the following prognostic (forward) 3 days calculations with the ADR model. During prognostic calculations, the hydrodynamic velocities and diffusivities change in accordance with the hydrodynamic model. The results of the Shulman *et al.* (2003) study suggested that it was more important to know the upstream boundary conditions in a highly advective environment than to have exact knowledge of the temporal distribution of the BP. In a follow-on study, the same model was used with more field data and there was close agreement between the observed and model-predicted downstream three dimensional distribution of bioluminescence (Shulman *et al.*, 2005). It was also demonstrated that optimization of the bioluminescence sampling strategy for the model initialization is critical for successful short-term predictions with the ADR model.

Although the benefits of integrating IOPs into dynamic models has been addressed (Fujii *et al.*, 2007), they have not been used to propagate bioluminescence. As measurements made in the case studies above (Sections 7.3.1 and 7.3.2) are technically difficult, the only way to apply these findings over large time and space scales is through modeling. Shulman *et al.* (2011a) was the first to attempt this: dynamical, predictive biochemical and bioluminescence intensity models were used to model and forecast the night-time water-leaving radiances (BL_w) due to stimulation of BP at depth. In the upwelling-driven system of Monterey Bay, CA, results



7.11 (Right) Water-leaving radiance at the surface due to stimulation of the modeled BL intensity at different depths (5, 15, and 25 m) on 15 August 2003. (middle) The modeled BL intensity for different depths of stimulations, and (left) a sum of absorption, a , and backscatter coefficient, b_b , averaged from the depth of BL stimulation to the surface.

showed that the offshore water masses with the subsurface layer of bioluminescent zooplankton were replaced by water masses advected from the northern coast of the Bay with a relatively high presence of mostly non-bioluminescent phytoplankton (Fig. 7.11). Offshore observations show a deeper BP maximum below the surface layers of high chlorophyll and backscatter values during the earlier stages of upwelling development. Later, the observed deep offshore BP maximum disappeared and became a shallower and much weaker signal. These dynamics influenced not only the BP in the region, but also the IOPs, a and b_b . Combining dynamical, predictive physical, biochemical and bioluminescence intensity models, Shulman *et al.* (2011a) was able to produce one of the first pictures of BL_w

for the entire region, illustrating the non-linearity of the quantity and the ocean circulation that, for the two components, is critical for estimation of BL_w on this scale (Fig. 7.11).

Finally, in a recent extension of this work, the advection–diffusion model was used to examine the persistence of dinoflagellates in Monterey Bay, CA, the site of the previous modeling efforts (Shulman *et al.*, 2011b). Here, the S term in Equation [78] was also used to incorporate the swimming behavior of dinoflagellates. Three swimming behaviors were considered: sinking, swimming to the target depth, and diel vertical migration. Results demonstrated that through swimming behavior, dinoflagellates avoid complete advection out of the Bay during upwelling events (Shulman *et al.*, 2011b). With a modeled swimming velocity of 20 m/day (a reasonable estimate at half the observed maximum) 40% of the dinoflagellates population was advected from the northern part of the Bay compared to no swimming. This is in agreement with the observed mean BP ratio of 0.45 at the Bay entrance compared to the northern part of the Bay. While some of the salient features of short-term changes in bioluminescence can be predicted and explained with the modeling of advective-diffusive processes, it was demonstrated (Shulman *et al.*, 2003, 2005, 2011a, 2011b) that the modeling of BL sources and sinks is needed to reproduce the observed spatial and temporal variability of the BL, even on short-time scales. Advective processes alone will not accurately predict even short-term changes in horizontal and vertical redistributions of bioluminescent populations. It is especially valid in situations where swimming behavior of bioluminescent plankton impacts the BL distribution. Continued modeling efforts such as these will gauge the measure of bioluminescence as a tool for integrating ecosystem information, evaluate dynamical optical properties in the ocean, and help in short-term prediction of oceanographic conditions, including BL_w .

7.4 Future trends

‘...great dazzling white patches that lighted and glittered like the stars.’

Don Joao de Castro, 1541

While limited in scope, this review has highlighted the diversity of bioluminescence in the ocean and the potential for bioluminescence measurements to better inform us of ocean function and dynamics. Bioluminescence is one of the primary forms of inter- and intra-species communication in the ocean. While such a dominant phenomenon, we know little of the chemistry of these reactions and biosynthetic pathways. Bioluminescence has widespread use in the medical field (i.e. imaging and bioassay for disease research) and for assaying pollution (Lapota *et al.*, 2007); however, these

applications originated from only a few bacterial species and bioreactivity molecules. Improved understanding of the diverse bioluminescent systems in nature can only increase the types and numbers of practical uses of bioluminescence. Bioluminescence communication in the ocean directly effects predator–prey interactions, the largest migration on the planet (DVM; Hays, 2003), and the flow of material through the food web. From an ecological perspective, these are some of the most difficult questions to address in the ocean today. The availability of instrumentation to measure BP and image bioluminescence now provides a complementary tool to investigate these challenging questions empirically and/or through modeling. Finally, the combination of IOPs and BP allow for the estimating of BL₁₀₀, the source depth, and source intensity at depth, providing an avenue for further investigation. With improved low-light sensors on above-water platforms (i.e. aircraft or satellites) and integration of *in situ* sensors of autonomous platforms (Moline *et al.*, 2005), we can now observe bioluminescence phenomena over increased spatial and temporal footprints. This is especially true if these observations and measurements are integrated into existing programs and/or observational networks (i.e. Schofield *et al.*, 2002). Given that bioluminescence serves as a dominant form of communication in the marine environment, it is prudent that investigation of this phenomenon be sustained to reveal its importance in the ocean.

7.5 Acknowledgements

Thanks to I. Robbins, S. Blackwell, and B. Selene for assistance in the field and with data analysis. Special thanks to S. Haddock for feedback and work on the previous bioluminescence review. This work was supported by funding from the Office of Naval Research (N00014–99–1–0197, N00014–00–1–0008, and N00014–03–1–0341) to M.A. Moline and (N00014–10–C-0272) to WetLabs, Inc. The writing was also supported through the Fulbright Arctic Chair supported by the Foreign Ministry of Norway.

7.6 References

- Abrahams V A and Townsend L D (1993), 'Bioluminescence in dinoflagellates: A test of the burglar alarm hypothesis', *Ecology*, **74**, 258–260.
- Aiken A and Kelley J (1984), 'A solid state sensor for mapping and profiling stimulated bioluminescence in the marine environment', *Cont Shelf Res*, **3**, 455–464.
- Alberte R S (1993), 'Bioluminescence: The fascination, phenomena, and fundamentals', *Nav Res Revs*, **45**, 2–12.
- Allen J I, Aiken J, Anderson T R, Buitenhuis E, Cornell S, Geider R J, Haines K, Hirata T, Holt J, Le Quéré C, Hardman-Mountford N, Ross O N, Sinha B and While J (2010), 'Marine ecosystem models for earth systems applications: The MarQUEST experience', *J Mar Sys*, **81**, 19–33.

- Backus R H, Yentch C S and Wing A S (1961), 'Bioluminescence in the surface waters of the sea', *Nature*, **205**, 989–991.
- Batchelder H P and Swift E (1988), 'Bioluminescence potential and variability in some Sargasso Sea planktonic halocypridostracods', *J Crustacean Biol*, **8**, 520–523.
- Batchelder H P, Swift E and van Keuren J R (1990), 'Pattern of planktonic bioluminescence in the northern Sargasso Sea: Seasonal and vertical distribution', *Mar Biol*, **104**, 153–164.
- Batchelder H P, Swift E and van Keuren J R (1992), 'Diel patterns of planktonic bioluminescence in the northern Sargasso Sea', *Mar Biol*, **113**, 329–339.
- Beebe W, Tee-Van J, Hollister G, Crane J and Barton O (1934), *Half Mile Down*, New York, Harcourt.
- Benoit-Bird K J, Moline M A, Waluk C M and Robbins I C (2010), 'Integrated measurements of acoustical and optical thin layers I: Vertical scales of association', *Continental Shelf Research*, **30**, 17–28. doi:10.1016/j.csr.2009.08.001.
- Berge J, Båtnes A S, Johnsen G, Blackwell S M and Moline M A (2012), 'Bioluminescence in the high arctic during the polar night', *Mar Biol*, **159**, 231–237, doi:10.1007/s00227-011-1798-0.
- Blackwell S M, Moline M A, Schaffner A, Garrison T and Chang G (2008), 'Sub-kilometer length scales in coastal waters', *Cont Shelf Res*, **28**, 215–226, doi:10.1016/j.csr.2007.07.009.
- Boden B P and Kampa E M (1974), 'Bioluminescence', in Jerlov N G and Nielsen S, eds., *Optical Aspects of Oceanography*, New York, Academic Press, 445–469.
- Bricaud A, Morel A and Prieur L (1983), 'Optical efficiency factors of some phytoplankters', *Limnol Oceanogr*, **28**, 816.
- Burkenroad M D (1943), 'A possible function of bioluminescence', *J Mar Res*, **5**, 161–164.
- Buskey E J (1992), 'Epipelagic planktonic bioluminescence in the marginal ice zone of the Greenland Sea', *Mar Biol*, **113**, 689–698.
- Carder K L, Lee Z P, Marra J, Steward R G and Perry M J (1995), 'Calculated quantum yield of photosynthesis of phytoplankton in the Marine Light-Mixed Layers (59°N, 21°W)', *J Geophys Res*, **100**, 6655–6664.
- Case J F, Widder E A, Bernsein S, Ferer K, Young D, Latz M I, Geiger M and Lapota D (1993), 'Assessment of marine bioluminescence', *Nav Res Revs*, **45**, 31–41.
- Clarke G L and Wertheim G K (1956), 'Measurements of illumination at great depths and at night in the Atlantic Ocean by means of a new bathyphotometer', *Deep-Sea Res*, **3**, 189–205.
- Clarke G L and Kelly M G (1965), 'Measurements of diurnal changes in bioluminescence from the sea surface to 2,000 meters using a new photometric device', *Limnol Oceanogr*, **10** (Redfield Suppl.), R54–R66.
- de Rada S, Arnone R A and Anderson S (2009), 'Bio-physical ocean modeling in the Gulf of Mexico', OCEANS 2009, *MTS/IEEE*, 1–7.
- Dickey T, Granata T, Marra J, Langdon C, Wiggert J, Chai-Jochner Z, Hamilton M, Vazquez J, Stramska M, Bidigare R and Siegel D (1993), 'Seasonal variability of bio-optical and physical properties in the Sargasso Sea', *J Geophys Res*, **98**, 865–898.
- Dickey T D and Chang G C (2001), 'Recent advances and future visions: Temporal variability of optical and bio-optical properties of the ocean', *Oceanogr*, **14**, 15–29.

- Doney S C, Lima I, Moore J K, Lindsay K, Behrenfeld M J, Westberry T K, Mahowald N, Glover D M and Takahashi T (2009), 'Skill metrics for confronting global upper ocean ecosystem-biogeochemistry models against field and remote sensing data', *J Mar Sys*, **76**, 95–112.
- Eckert R and Reynolds G T (1967), 'The subcellular origin of bioluminescence in *Noctiluca miliaris*', *J Gen Physiol*, **50**, 1429–1458.
- Fucile P D (1996), 'A low cost bioluminescence bathyphotometer', Gulf of Maine Ecosystems Dynamics Symposium, NOAA, St Andrew's, New Brunswick, Canada, 11–16 September.
- Fucile P D, Widder E and Brink K (2001), 'A compact bathyphotometer', ONR Final Report, N00014–99–1–0346.
- Fujii M, Boss E and Chai F (2007), 'The value of adding optics to ecosystem models: a case study', *Biogeosciences*, **4**, 817–835.
- Geistdoerfer P and Vincendeau M-A (1999), 'A new bathyphotometer for bioluminescence measurements on the Armorican continental shelf (northeastern Atlantic)', *Oceanologica Acta*, **22**, 137–151.
- Geistdoerfer P and Cussatlegras A-S (2001), 'Day/night variations of marine bioluminescence in the Mediterranean Sea and in the northeastern Atlantic', *C. R. Acad. Sci. Paris*, **324**, 1037–1044.
- Gillibrand E J V, Bagley P, Jamieson A, Herring P J, Partridge J C, Collins M A, Milne R and Priede I G (2007a), 'Deep sea benthic bioluminescence at artificial food falls, 1000–4800 m depth, in the Porcupine Seabight and Abyssal Plain, North East Atlantic Ocean', *Mar Biol*, **150**, 1053–1060.
- Gillibrand E, Jamieson A, Bagley P, Zuur A and Priede I (2007b), 'Seasonal development of a deep pelagic bioluminescent layer in the temperate NE Atlantic Ocean', *Mar Ecol Prog Ser*, **341**, 37–44.
- Gordon H R (1984), 'Remote sensing marine bioluminescence: The role of the in-water scaler irradiance', *Appl Opt*, **23**, 1694–1696.
- Gordon H R (1987), 'Bio-optical model describing the distribution of irradiance at the sea surface resulting from a point source embedded in the ocean', *Appl Opt*, **26**, 4133–4148.
- Haddock S H D, Rivers T J and Robison B H (2001), 'Can coelenterates make coelenterazine? Dietary requirement for luciferin in cnidarian bioluminescence', *Proc Natl Acad Sci USA*, **98**, 11148–11151.
- Haddock S H D, Moline M A and Case J F (2010), 'Bioluminescence in the sea', *Annu Rev Mar Sci*, **2**, 443–493.
- Haidvogel D B, Blanton J, Kindle J C and Lynch D R (2000), 'Coastal ocean modeling: Processes and real-time systems', *Oceanogr*, **13**, 35–46.
- Hays G C (2003), 'A review of the adaptive significance and ecosystem consequences of zooplankton diel vertical migrations', *Hydrobiologia*, **503**, 163–170.
- Herren C M, Haddock S H D, Johnson C, Orrico C M, Moline M A and Case J F (2005), 'A multi-platform bathyphotometer for fine-scale, coastal bioluminescence research', *Limnol Oceanogr Methods*, **3**, 247–262.
- Herring P J (1978), 'A classification of luminous organisms', in Herring P J, ed., *Bioluminescence in Action*, New York, Academic Press, 461–476.
- Herring P J (1987), 'Systematic distribution of bioluminescence in living organisms', *J Biol Chem*, **1**, 147–163.
- Jerlov N G (1976), *Marine Optics*, Amsterdam, Elsevier.

- Jerlov N G and Nielsen S (1974), *Optical Aspects of Oceanography*, New York, Academic Press.
- Kampa E M and Boden B P (1953), 'Light generation in a sonic-scattering layer', *Deep-Sea Res*, **4**, 73–92.
- Kim G, Lee Y-W, Joung D-J, Kim K-R and Kim K (2006), 'Real-time monitoring of nutrient concentrations and red-tide outbreaks in the southern sea of Korea', *Geophys Res Lett*, **33**, L13607, doi:10.1029/2005GL025431.
- Lapointe M and Morse D (2008), 'Reassessing the role of a 3%-UTR-binding translational inhibitor in regulation of circadian bioluminescence rhythm in the dinoflagellate *Gonyaulax*', *Biol Chem*, **389**, 13–19.
- Lapota D (1998), 'Long term and seasonal changes in dinoflagellate bioluminescence in the Southern California Bight', Ph.D. Dissertation, University of California Santa Barbara, Santa Barbara, CA.
- Lapota D and Losee J R (1984), 'Observations of bioluminescence in marine plankton from the Sea of Cortez', *J Exp Mar Biol Ecol*, **77**, 209–240.
- Lapota D, Galt C, Losee J, Huddell H D, Orzech J K and Neelson K H (1988), 'Observations and measurements of planktonic bioluminescence in and around a milky sea', *J Exp Mar Biol Ecol*, **119**, 55–81.
- Lapota D, Osorio A R, Liao C and Bjorndal B (2007), 'The use of bioluminescent dinoflagellates as an environmental risk assessment tool', *Mar Poll Bull*, **54**, 1857–1867.
- Lapota, D, Rosenberger D E and Lieberman S H (1992a), 'Planktonic bioluminescence in the pack ice and the marginal ice zone of the Beaufort Sea', *Mar Biol*, **112**, 665–675.
- Lapota D, Young D, Bernstein S, Geiger M, Huddell H D L and Case J F (1992b), 'Diel bioluminescence in heterotrophic and photosynthetic marine dinoflagellates in an Arctic fjord', *J Mar Biol Assoc U K*, **72**, 733–744.
- Latz M I, Frank T M, Bowlby M R, Widder E A and Case J F (1987), 'Variability in flash characteristics of a bioluminescent copepod', *Biol Bull*, **162**, 423–448.
- Levin L A, Utyushev R N and Artemkin A S (1977), 'Distribution of bioluminescence in the equatorial waters of the eastern Pacific Ocean', *Polskie Archwm Hydrobiol*, **24**, 125–134.
- Lieberman S H, Lapota D, Losee J R and Zirino A (1987), 'Planktonic bioluminescence in the surface waters of the Gulf of California', *Biol Oceanogr*, **4**, 25–46.
- Losee J, Lapota D and Lieberman S H (1985), 'Bioluminescence: A new tool for oceanography', in Zirion A, *Mapping Strategies in Chemical Oceanography*, *Adv Chem Ser*, 209, Washington D.C., American Chemical Society.
- Lynch R V (1981), 'Patterns of bioluminescence in the oceans', NRL Report 8475, Washington D.C., Naval Research Laboratory.
- Maffione R A, Voss K J and Honey R C (1993), 'Measurement of the spectral absorption coefficient in the ocean with an isotropic light source', *Appl Opt*, **32**, 3273–3279.
- Marra J (1984), *Biowatt: A Study of Bioluminescence and Optical Variability in the Sea*, Palisades, NY, Lamont-Doherty Geological Observatory.
- Marra J and Hartwig E O (1984), 'Biowatt: A study of bioluminescence and optical variability in the sea', *EOS*, **65**, 732–733.
- Marra J, Langdon C and Knudson C A (1995), 'Primary production, water column changes, and the demise of a *Phaeocystis* bloom at the Marine Light-Mixed

- Layer site (59°N, 21°W) in the northeast Atlantic Ocean', *J Geophys Res*, **100**, 6633–6643.
- Mensingher A F and Case J F (1992), 'Dinoflagellate luminescence increases susceptibility of zooplankton to teleostpredation', *Mar Biol*, **112**, 207–210.
- Menzel D W (1967), 'Particulate organic carbon in the deep sea', *Deep-Sea Res*, **14**, 229–238.
- Miller S D, Haddock S H D, Elvidge C D and Lee T H (2005), 'Detection of a bioluminescent milky sea from space', *Proc Natl Acad Sci USA*, **102**, 14181–14184.
- Mobley C D (1994), *Light and Water: Radiativetransfer in Natural Waters*, New York, Academic Press.
- Moline M A, Blackwell S M, Allen B, Austin T, Forrester N, Goldsborough R, Purcell M, Stokey R and von Alt C (2005), 'Remote environmental monitoring units: An autonomous vehicle for characterizing coastal environments', *J Atmos Oceanic Technol*, **22**, 1798–1809.
- Moline M A, Oliver M J, Mobley C D, Sundman L, Bensky T, Bergmann T, Bissett W P, Case J, Raymond E H and Schofield O M E (2007), 'Bioluminescence in a complex coastal environment: 1. Temporal dynamics of nighttime water-leaving radiance', *J Geophys Res*, **112**, C11016, doi:10.1029/2007JC004138.
- Moline M A, Blackwell S M, Case J F, Haddock S H D, Herren C M, Orrico C M and Terrill E (2009), 'Bioluminescence to reveal structure and interaction of coastal planktonic communities', *Deep-Sea Res*, **56**, 232–245, doi:10.1016/j.dsr.2008.08.002.
- Moline M A, Benoit-Bird K J, Robbins I C, Schroth-Miller M, Waluk C M and Zelenke B (2010), 'Integrated measurements of acoustical and optical thin layers II: Horizontal length scales', *Continental Shelf Research*, **30**, 29–38, doi:10.1016/j.csr.2009.08.004.
- Morel A and Prieur L (1977), 'Analysis of variations in ocean color', *Limnol Oceanogr*, **22**, 709.
- Moore C, Zaneveld J R V, and Kitchen J C (1992), 'Preliminary results from an *in situ* spectral absorption meter', in Gilbert G D, *Ocean Optics XI, Proc. SPIE*, **1750**, 330–337.
- Morin J G (1983), 'Coastal bioluminescence: Patterns and functions', *Bull Mar Sci*, **33**, 787–817.
- Morin J G and Bermingham E L (1980), 'Bioluminescent patterns in atropical ostracod', *Amer Zool*, **20**, 851.
- Morin J G and Cohen A C (1991), 'Bioluminescent displays, courtship, and reproduction in ostracodes', in Bauer R and Martin J, eds., *Crustacean Sexual Biology*, New York, Columbia University Press.
- Morin J G and Cohen A C (2010), 'It's all about sex: Bioluminescent courtship displays, morphological variation and sexual selection in two new genera of Caribbeanostracods', *J Crustacean Biol*, **30**, 56–67.
- Morse D S, Fritz L and Hastings J W (1990), 'What is the clock? Translational regulation of circadian bioluminescence', *Trends in Biochemical Sciences*, **15**, 262–265.
- Nakamura H, Kishi Y, Shimomura O, Morse D and Hastings J W (1989), 'Structures of dinoflagellateluciferin and its enzymatic and non-enzymatic air-oxidation products', *J Am Chem Soc*, **111**, 7607–7611.
- Nealson K H, Arneson A C and Bratkovich A (1984), 'Preliminary results from studies of nocturnal bioluminescence with subsurface moored photometers', *Mar Biol*, **83**, 185–191.

- Nelson CV (1985), *Bio-optical Measurement Platforms and Sensors*, JHU/APL Tech. Rep. STD-R-1160, Laurel, Johns Hopkins University.
- Ocean Studies Board, National Research Council (1997) *Oceanography and Naval Special Warfare: Opportunities and Challenges*, Washington D.C., National Academy Press.
- Oliver M J, Moline M A, Mobley C D, Sundman L and Schofield O M E (2007), 'Bioluminescence in a complex coastal environment: 2. Prediction of bioluminescent source depth from spectral water-leaving radiance', *J Geophys Res*, **112**, C11017, doi:10.1029/2007JC004136.
- Ondercin D G, Atkinson C A and Kiefer D A (1995), 'The distribution of bioluminescence and chlorophyll during the late summer in the North Atlantic: Maps and a predictive model', *J Geophys Res*, **100**, 6575–6590.
- Orrico C M, Moline M A, Robbins I, Zelenke B, Barnard A H, Strubhar W, Koepler J and Moore C (2010), 'A new tool for monitoring ecosystem dynamics in coastal environments: Long-term use and servicing requirements of the commercial Underwater Bioluminescence Assessment Tool (U-BAT)', *Oceans 2009, MTS/IEEE*, 1–7.
- Orrico C M, Zaneveld J R V, Moline M A, Robbins I and Barnard A H (2013), 'Measured and modeled nighttime visibility of vehicle stimulated bioluminescence (U)', *J Underwater Acoustics*, in press.
- Petzold T J (1972), 'Volume Scattering Functions for Selected Natural Waters', Scripps Institute of Oceanography, Visibility Laboratory, San Diego, CA 92152, SIO Ref. 72–78.
- Piontkovski S A, Tokarev Y N, Bitukov E P, Williams R and Kiefer D A (1997), 'The bioluminescent field of the Atlantic Ocean', *Mar Ecol Prog Series*, **156**, 33–41.
- Priede I G, Bagley P M, Way S, Herring P J and Partridge J C (2006), 'Bioluminescence in the deep sea: Free-fall lander observations in the Atlantic Ocean off Cape Verde', *Deep-Sea Res*, **53**, 1272–1283.
- Rees J F, DeWergifosse B, Noiset O, Dubuisson M, Janssens B and Thompson E M (1998), 'The origins of marine bioluminescence: Turning oxygen defense mechanisms into deep-sea communication tools', *J Exp Biol*, **201**, 1211–1221.
- Reynolds G T (1964), 'Evaluation of an image intensifier system for microscopic observations', *IEEE Trans Nucl Sci*, **11**, 147.
- Rivers T J and Morin J G (2008), 'Complex sexual courtship displays by luminescent male marine ostracods', *J Exp Biol*, **211**, 2252–2262.
- Rohr J, Latz M I, Fallon S, Nauen J C and Hendricks E (1998), 'Experimental approaches towards interpreting dolphin-stimulated bioluminescence', *J Exp Biol*, **201**, 1447–1460.
- Roithmayr C M (1970), 'Airborne low-light sensor detects luminescing fish schools at night', *Commer Fish Rev*, **32**, 42–51.
- Schofield O, Bergmann T, Bissett P, Grassle J F, Haidvogel D B, Kohut J, Moline M A and Glenn S M (2002), 'The long-term ecosystem observatory: An integrated coastal observatory', *IEEE J Oceanic Eng*, **27**, 146–154.
- Seliger H H (1993), 'Bioluminescence: Excited states under the cover of darkness', *Nav Res Rev*, **45**, 5–11.
- Seliger H H, Fastie W G, Taylor W R and McElroy W D (1963), 'Bioluminescence of marine dinoflagellates. I. An underwater photometer for day and night measurements', *J Gen Physiol*, **45**, 1003–1017.

- Seliger H H, Fastie W G and McElro W D (1969), 'Towable photometer for rapid area mapping of concentrations of bioluminescent marine dinoflagellates', *Limnol Oceanogr*, **14**, 806–813.
- Shulman I, Haddock S H D, McGillicuddy Jr. D J, Paduan J D and Bissett W P (2003), 'Numerical modeling of bioluminescence distributions in the coastal ocean', *J Atmos Oceanic Technol*, **20**, 1060–1068.
- Shulman I, McGillicuddy Jr. D J, Moline M A, Haddock S H D, Kindle J C, Nechaev D and Phelps M W (2005), 'Bioluminescence intensity modeling and sampling strategy optimization', *J Atmos Oceanic Technol*, **22**, 1267–1281.
- Shulman I, Moline M A, Penta B, Anderson S, Oliver M and Haddock S H D (2011a), 'Observed and modeled bio-optical, bioluminescent, and physical properties during a coastal upwelling event in Monterey Bay, California', *J Geophys Res*, **116**, C01018, doi:10.1029/2010JC006525.
- Shulman I, Penta B, Moline M A, Haddock S H D, Anderson S, Oliver M J and Sakalaukus P (2011b), 'Can vertical migrations of dinoflagellates explain observed bioluminescence patterns during an upwelling event in Monterey Bay, CA?', *J Geophys Res*, **117**, C01016, doi:10.1029/2011JC007480, in press.
- Smith R C and Baker K S (1978), 'Optical classification of natural waters', *Limnol Oceanogr*, **23**, 260.
- Smith R C, Marra J, Perry M J, Baker K S, Swift E, Buskey E and Kiefer D A (1989), 'Estimation of a photon budget for the upper ocean in the Sargasso Sea', *Limnol Oceanogr*, **34**, 1673–1693.
- Smith S M E, Morgan D, Musset B, Cherny V V, Place A R, Hastings J W and DeCoursey T E (2011), 'Voltage-gated proton channel in a dinoflagellate', *Proc Natl Acad Sci USA*, **108**, 18162–18167.
- Soli G (1966), 'Bioluminescent cycle of photosynthetic dinoflagellates', *Limnol Oceanogr*, **11**, 355–363.
- Stephany S, Campos Velho H F, Ramos F M and Mobley C D (2000), 'Identification of inherent optical properties and bioluminescence source term in a hydrological optics problem', *J Quant Spectroscopy Radiative Transfer*, **67**, 113–123.
- Stramska M, Dickey T D, Plueddemann A, Weller R, Langdon C and Marra J (1995), 'Bio-optical variability associated with phytoplankton dynamics in the North Atlantic Ocean during spring and summer of 1991', *J Geophys Res*, **100**, 6621–6632.
- Swift E, Lessard E J and Biggley W H (1985), 'Organisms associated with stimulated epipelagic bioluminescence in the Sargasso Sea and the Gulf Stream', *J Plank Res*, **7**, 831–848.
- Swift E, Sullivan J M, Batchelder H P, van Keuren J, Vaillancourt R D and Bidigare R R (1995), 'Bioluminescent organisms and bioluminescence measurements in the North Atlantic Ocean near latitude 59.5°N, longitude 21°W', *J Geophys Res*, **100**, 6527–6547.
- Utyushev R N, Levin L A and Gitelson J I (1999), 'Diurnal rhythm of the bioluminescent field in the ocean epipelagic zone', *Mar Biol*, **134**, 439–448.
- Vinogradov M E, Gittelzon I I and Sorokin Y I (1970), 'The vertical structure of a pelagic community in the tropical ocean', *Mar Biol*, **6**, 187–194.
- Ward W W and Seliger H H (1974), 'Properties of mnemiopsin and berovin, calcium-activated photoproteins from the ctenophores *Mnemiopsis* sp. and *Beroeovata*', *Biochemistry*, **13**, 1500–1509.

- Widder E A (1997), 'Bioluminescence', *Sea Tech*, **3**, 33–39.
- Widder E A (2002), 'Bioluminescence and the pelagic visual environment', *Mar Freshwater Behav Physiol*, **35**, 1–26.
- Widder E A (2010), 'Bioluminescence in the ocean: Origins of biological, chemical and ecological diversity', *Science*, **328**, 704–708.
- Widder E A and Case J F (1981), 'Bioluminescence excitation in a dinoflagellate', in Nealon K H, ed., *Bioluminescence Current Perspectives*, Burgess, Burgess Publishing, 125–132.
- Widder E A and Johnsen S (2000), '3D spatial point patterns of bioluminescent-plankton: a map of the "minefield"', *J Plank Res*, **22**, 409–420.
- Widder E A, Bernstein S A, Bracher D F, Case J F, Reisenbichler K R, Torres J J and Robison B H (1989), 'Bioluminescence in the Monterey Submarine Canyon: Image analysis of video recordings from a midwater submersible', *Mar Biol*, **100**, 541–551.
- Widder E A, Case J F, Bernstein S A, MacIntyre S, Lowenstine M R, Bowlby M R and Cook D P (1993), 'A new large volume bioluminescence bathyphotometer with defined turbulence excitation', *Deep-Sea Res*, **40**, 607–627.
- Widder E A, Johnson S, Bernstein S A, Case J F and Neilson D J (1999), 'Thin layers of bioluminescent copepods found at density discontinuities in the water column', *Mar Biol*, **134**, 429–437.
- Williamson C E, Fischer J M, Bollens S M, Overholt E P and Breckenridge J K (2011), 'Toward a more comprehensive theory of zooplankton diel vertical migration: Integrating ultraviolet radiation and water transparency into the biotic paradigm', *Limnol Oceanogr*, **56**, 1603–1623.
- Wren G G and May D (1997), 'Detection of submerged vessels using remote sensing', *Techniques Australian Defense Forces Journal*, **127**, 9–15.
- Yi H C, Sanchez R and McCormick N J (1992), 'Bioluminescence estimation from ocean *in situ* irradiances', *Appl Optics*, **31**, 822–830.
- Zaneveld J R V, Kitchen J C and Moore C C (1994), 'Scattering error correction of reflecting tube absorption meters', in Ackleson S, *Ocean Optics XII, Proc. SPIE*, **2258**, 44–55.
- Zaneveld J R V and Pegau W S (2003), 'Robust underwater visibility parameter', *Optics Express*, **11**, 2997–3009.